

Dipole excitations in the transitional nucleus ^{144}Nd studied in photon scattering experiments

T. Eckert,¹ O. Beck,¹ J. Besserer,¹ P. von Brentano,² R. Fischer,² R.-D. Herzberg,² U. Kneissl,¹ J. Margraf,¹ H. Maser,¹ A. Nord,¹ N. Pietralla,² H. H. Pitz,¹ S. W. Yates,³ and A. Zilges²

¹*Institut für Strahlenphysik, Universität Stuttgart, Allmandring 3, D-70569 Stuttgart, Germany*

²*Institut für Kernphysik, Universität zu Köln, Zùlpicher Str. 77, D-50937 Köln, Germany*

³*Department of Chemistry, University of Kentucky, Lexington, Kentucky 40506-0055*

(Received 4 April 1997)

Low-lying electric and magnetic dipole excitations in the transitional nucleus ^{144}Nd have been studied in nuclear resonance fluorescence experiments performed with a bremsstrahlung beam (end point energy 4.1 MeV). The use of high-resolution γ -ray spectrometers and a sectored single-crystal Compton polarimeter provided detailed information on excitation energies, spins, parities, decay widths, transition probabilities, and branching ratios of numerous new spin-1 states in ^{144}Nd . The strong $E1$ excitation at 2185 keV in this $N = 84$ nucleus is interpreted as the quadrupole-octupole coupled two-phonon excitation which has been observed systematically in the neighboring $N = 82$ isotones. The decay properties of this 1^- state are compared with the systematics of the low-lying 1^- levels in the other even-even, stable Nd isotopes. The $M1$ excitations in ^{144}Nd are discussed with respect to the deformation dependence of the orbital $M1$ "scissors mode," the so-called " δ^2 law," which has been studied previously in the other stable even-even Nd nuclei and in the Sm isotopes. [S0556-2813(97)00609-2]

PACS number(s): 25.20.Dc, 21.10.Re, 23.20.-g, 27.60.+j

I. INTRODUCTION

The transitional nucleus ^{144}Nd with two neutrons outside the closed $N=82$ shell has a small deformation (deformation parameter $\delta=0.114$ or $\beta_2=0.1309$ [1,2]), and it provides an interesting laboratory for the study of different low-lying dipole excitation mechanisms of both electric and magnetic character. A common feature in the neighboring semimagic $N=82$ isotones is a strong $E1$ excitation near to the sum of the excitation energies of the quadrupole (2^+) and octupole (3^-) vibrations [3-9]. In ^{144}Nd the effect of the two neutrons outside the closed shell on the excitation strengths and the decay properties of the corresponding 1^- level can be studied.

In addition, ^{144}Nd is a member of the chain of stable even-even Nd isotopes which represents an ideal case for studying the influence of the shape transition from spherical to deformed nuclei on nuclear excitation modes, e.g., the orbital $M1$ scissors mode. The deformation dependence of this mode has been studied in the Sm chain by the Darmstadt group [10,11] and in the Nd chain ($^{142,146,148,150}\text{Nd}$) at the Stuttgart facility [12]. However, it should be emphasized that for the interpretation of the results of such nuclear resonance fluorescence (NRF) experiments, parity assignments are crucial. Parities can be determined in NRF studies by measuring the linear polarization of the scattered photons with a Compton polarimeter. Such measurements have been performed at Stuttgart for $^{142,150}\text{Nd}$ [13-15] and ^{146}Nd [16]. Therefore, an important aim of the present study was to perform polarization measurements and to obtain reliable parity assignments for an additional, yet critical Nd isotope.

Because of the spin selectivity of the real photon probe, the NRF technique has proved to be the most sensitive tool for the investigation of low-lying dipole excitations of both electric and magnetic character and detailed nuclear structure information is obtained in a completely model-independent

way [17,18]. Precise excitation energies E_x , ground-state transition widths Γ_0 , total widths Γ , reduced excitation probabilities $B(E1)\uparrow$ or $B(M1)\uparrow$, decay branching ratios R_{expt} , and spins and parities of the excited states can be extracted. The formalism describing this classical method can be found in recent reviews [17,18].

In the next subsections the physical motivation for this work is outlined in greater detail. Section II then deals with the description of the experimental technique and the setup. After a presentation of the results in Sec. III, these results are compared with previous data in Sec. IV and discussed in the framework of appropriate theoretical concepts.

A. $E1$ excitations to quadrupole-octupole coupled states

In vibrational nuclei, coupling between the quadrupole and octupole phonons is expected to produce a quintuplet of negative-parity states (1^- to 5^-) [19,20]. In a recent review of nuclear structures that could be populated by resonance fluorescence scattering, the evidence for quadrupole-octupole coupled states in even- A nuclei near $N = 82$ was assessed [17]. In summary, the spectra of all of the stable even-even $N = 82$ nuclei studied with the (γ, γ') reaction are dominated by an isolated strong transition from a 1^- state at about 3.5 MeV to the ground state, the energies of these 1^- excitations are nearly harmonic, i.e., close to the sum of the energies of the quadrupole and octupole phonons, and the absolute $E1$ transition strength to the ground state is rather constant and strong, about 3×10^{-3} Weisskopf units (W.u.) (see, e.g., [7]). These states have long been interpreted [21] as the lowest-spin members of the $2^+ \otimes 3^-$ two-phonon quintuplet, and quasiparticle-phonon model (QPM) calculations [22] reproduce the observed transition strengths reasonably well. Moreover, the recent observation of the expected one-phonon decays to the 2^+ quadrupole phonon [8,9] and the 3^- octupole phonon [9] with transition rates

consistent with the phonon coupling picture add additional credence to the interpretation of these 1^- states as quadrupole-octupole coupled excitations. While candidates for other members of the quintuplet have been suggested [6] on the basis of fast $E1$ transitions, these states have not been conclusively identified in $N = 82$ nuclei. These two-phonon $E1$ excitations seem to be a rather common feature in heavy, semimagic nuclei and have also been observed consistently in the Sn isotopes ($Z=50$) [23]. The enhanced $E1$ strengths can be explained by including one-particle-one-hole (1p-1h) admixtures at the tail of the electric giant dipole resonance (GDR) into the collective two-phonon states [23,24].

In $N = 84$ nuclei, with the addition of two neutrons to the closed shell, the energies of the quadrupole phonons drop dramatically as their collectivity increases; however, a persistent feature observed in (γ, γ') spectra of both ^{142}Ce [25] and ^{144}Nd [26] is the strong excitation of a 1^- state at an energy near the sum of the quadrupole and octupole phonons. As in the $N = 82$ nuclei, this excitation in ^{144}Nd is, quite naturally, interpreted as a $(2^+ \otimes 3^-)$ two-phonon excitation.

B. $M1$ excitations of the scissors mode

The prediction [27] and subsequent discovery [28] of a low-lying, enhanced $M1$ excitation in deformed nuclei, the so-called *scissors mode*, was one of the most exciting observations in nuclear spectroscopy during the last decade. Now well known from numerous photon and electron scattering experiments (see, e.g., recent reviews [17,29] for references), the common features of this predominantly orbital mode are a mean excitation energy of about 3 MeV (in deformed rare earth nuclei) and a total strength $\Sigma B(M1)\uparrow$ on the order of $3 \mu_N^2$ for midshell rare earth nuclei. Another interesting property of the *scissors mode* is its deformation dependence.

The stable even-even nuclei in the Sm and Nd isotopic chains represent excellent opportunities for studying the behavior of the total low-lying $M1$ strengths in the transitional region from spherical to deformed nuclei. The shape transition within these isotopic chains, starting from the spherical $N = 82$ isotones (^{144}Sm , ^{142}Nd) and ending at the deformed nuclei (^{154}Sm , ^{150}Nd), is nicely illustrated by the deformation splitting of the GDR [30,31]. Another criterion for the shape transition is the behavior of the ratio of the energies of the first 4^+ and 2^+ states; e.g., the theoretical E_{4^+}/E_{2^+} ratio changes from 2 for spherical vibrators to 10/3 for good rotors.

The shape transition and its influence on the orbital $M1$ strength have been investigated in detail through systematic NRF experiments on even-even Nd nuclei ($^{142,146,148,150}\text{Nd}$) at the Stuttgart Dynamitron [12,16] and on the Sm isotopes ($^{144,148,150,152,154}\text{Sm}$) at the Darmstadt S-DALINAC [10,11], respectively. In the latter experiment the Darmstadt group showed for the first time that the total orbital $M1$ strength increases proportionally to the square of the deformation parameter δ , an effect often referred to as the “ δ^2 law.” This deformation dependence then could be confirmed by parity determinations (via polarization measurements) of the corresponding dipole excitations in the $^{142,146,150}\text{Nd}$ nuclei [13–15]. Additional, precise NRF measurements (including polarization measurements) in nearly spherical nuclei like

^{144}Nd are of interest for studying this correlation in the mass region of the shape transition.

II. EXPERIMENTAL METHOD

A. Nuclear resonance fluorescence technique

In the following paragraphs the relations needed for the discussion of the present NRF results are briefly summarized. In NRF experiments using continuous bremsstrahlung the photon scattering cross sections from bound nuclear states at an excitation energy E_x can be measured. The total scattering intensity I_s , the cross section integrated over one resonance, and the full solid angle

$$I_s = g \left(\pi \frac{\hbar c}{E_x} \right)^2 \frac{\Gamma_0 \Gamma_f}{\Gamma} \quad (1)$$

are determined absolutely [17,18]. Γ_0 , Γ_f , and Γ are the decay widths of the excited state with spin J to the ground state with spin J_0 , to the final level, and the total level width, respectively. The so-called spin factor $g = (2J+1)/(2J_0+1)$ is equal to 3 in the case of dipole excitations in even-even nuclei. $g\Gamma_0$ is related to the reduced excitation probabilities $B(\Pi L, E_x)\uparrow = B(\Pi L; J_0 \rightarrow J(E_x))$ ($\Pi = E$ or M) by

$$g\Gamma_0 = 8\pi \sum_{\Pi L=1}^{\infty} \frac{L+1}{L[(2L+1)!!]^2} \left(\frac{E_x}{\hbar c} \right)^{2L+1} B(\Pi L, E_x)\uparrow. \quad (2)$$

For pure dipole transitions, the reduced dipole excitation probability

$$B(\Pi 1)\uparrow = g B(\Pi 1)\downarrow = \frac{9}{16\pi} \left(\frac{\hbar c}{E_x} \right)^3 (g\Gamma_0) \quad (3)$$

can be calculated from the measured quantity $g\Gamma_0$. In practice, the following numerical relations are useful for electric or magnetic dipole excitations, respectively:

$$B(E1)\uparrow = \frac{2.866}{3} \frac{g\Gamma_0}{E_x^3} [10^{-3} e^2 \text{ fm}^2], \quad (4)$$

$$B(M1)\uparrow = \frac{0.2592}{3} \frac{g\Gamma_0}{E_x^3} [\mu_N^2]. \quad (5)$$

Here the excitation energies E_x are in MeV and the ground-state transition widths Γ_0 in meV .¹

Measurements of the angular distributions of the scattered photons provide the spins J of the photoexcited levels (unambiguously in the case of even-even nuclei) [17,18]. The theoretical intensity ratio $W(\Theta = 90^\circ)/W(\Theta = 127^\circ)$ is 0.734 and 2.28 for dipole and quadrupole transitions, respectively.

¹In some of our previous work [17,32,33] in the text, not used in the evaluations, a slightly different scaling factor of 0.2598 was given in Eq. (5), due to rounding errors.

These values are slightly reduced for realistic geometries used in the experiments due to the finite solid angles of the detectors.

For parity assignments, which are crucial for the interpretation of the results, the linear polarization of the scattered photons must be measured, e.g., by using a Compton polarimeter [17,34]. Parity information then is obtained from the measured azimuthal asymmetry ε ,

$$\varepsilon = \frac{N_{\perp} - N_{\parallel}}{N_{\perp} + N_{\parallel}} = P_{\gamma} \cdot Q, \quad (6)$$

where N_{\perp} and N_{\parallel} represent the rates of Compton scattered events perpendicular and parallel to the NRF scattering plane, defined by the directions of the incoming photon beam and the scattered photons, respectively. The asymmetry ε is given by the product of the polarization sensitivity Q of the polarimeter and the degree of polarization P_{γ} of the scattered photons. At a scattering angle of $\Theta = 90^{\circ}$ to the beam axis the polarization P_{γ} is -1 or $+1$ for pure $E1$ and $M1$ excitations, respectively (0-1-0 spin sequences). Therefore, the sign of the asymmetry ε obviously can be used to determine the parity.

For the discussion of transitions where the parity cannot be determined, we introduce the quantity $g\Gamma_0^{\text{red}}$, which is proportional to the corresponding reduced ground-state transition probabilities $B(\Pi 1) \uparrow$ [see Eqs. (4) and (5)]:

$$g\Gamma_0^{\text{red}} = g \frac{\Gamma_0}{E_x^3}. \quad (7)$$

The photoexcited states can decay back to the ground state (spin J_0) or to another low-lying excited level (spin J_f). The corresponding decay branching ratio R_{expt} is defined as

$$R_{\text{expt}} = \frac{B(\Pi L; J \rightarrow J_f)}{B(\Pi L; J \rightarrow J_0)} = \frac{\Gamma_f E_{\gamma J_0}^3}{\Gamma_0 E_{\gamma J_f}^3}. \quad (8)$$

It should be emphasized that for deformed nuclei the branching ratio R_{expt} provides valuable information on the K quantum number K of the excited state, if the validity of the so-called Alaga rules [48] is assumed.

B. Experimental setup

The present NRF experiments were performed at the well-established bremsstrahlung facility installed at the 4.3 MeV Dynamitron accelerator of the University of Stuttgart. The facility has been described in detail [17,32,35]. The accelerator delivers a dc electron beam with an energy $E_e = 4.1$ MeV at a maximum current of 4 mA; however, the thermal capacity of the water-cooled radiator target used for bremsstrahlung production limited the usable intensity of the electron beam in the present NRF experiments to about 250 μA . The collimated bremsstrahlung beam struck the nuclear scattering sample which consisted of 5934 mg of Nd oxide (Nd_2O_3) enriched to 97.51% in ^{144}Nd (the major impurities were 0.85% of ^{145}Nd , 0.66% of ^{143}Nd , 0.46% of ^{142}Nd , and 0.39% of ^{146}Nd). The Nd_2O_3 powder was pressed into pellets which were sandwiched by Al disks (total mass 2803

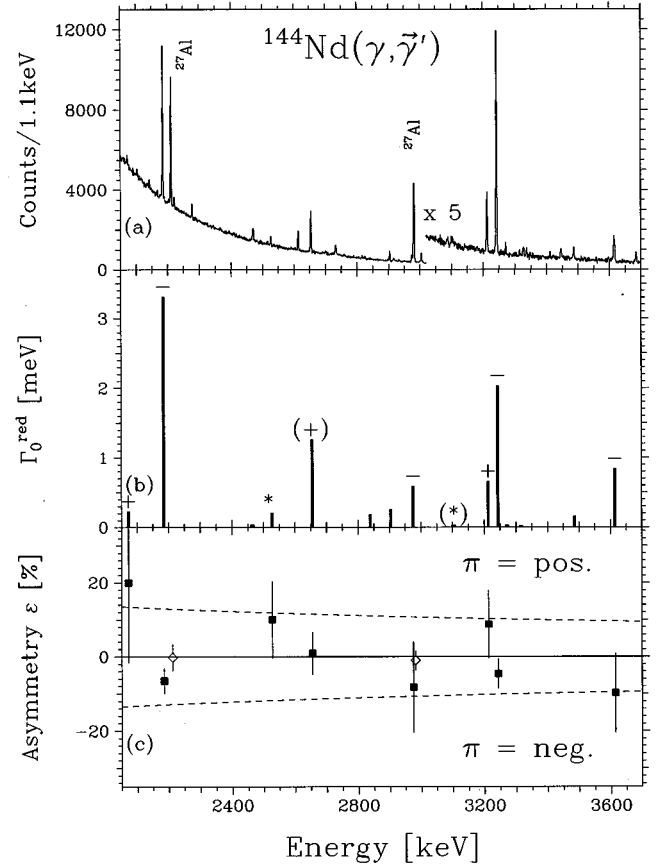


FIG. 1. Experimental results for photon scattering and polarization measurements on ^{144}Nd . Upper panel: spectrum of scattered photons measured with the BGO-shielded Compton polarimeter. Middle panel: reduced ground-state decay widths Γ_0^{red} of the photoexcited levels. Parity assignments are given, and tentative parity assignments are shown in parentheses. Lower panel: azimuthal asymmetries ε measured with the Compton polarimeter together with the anticipated values for completely polarized scattered photons (dashed lines). Solid squares belong to transitions in ^{144}Nd , and open diamonds correspond to nearly unpolarized photons from transitions in the photon flux monitor ^{27}Al .

mg). The well-known transitions in ^{27}Al served as an absolute photon flux monitor [36]. The scattered photons were detected by a high-resolution Ge detector installed at 128° with respect to the incident bremsstrahlung beam and a fourfold-sectored single-crystal Ge-Compton polarimeter [34] at 98° . The efficiencies of the γ -ray detectors, relative to a standard 7.6 cm \times 7.6 cm NaI(Tl) detector, were 31% (detector at 128°) and 25% for the polarimeter. The Compton polarimeter has a polarization sensitivity Q of about 20% for photons of an energy of 0.5 MeV and about 10% for photons of 4.4 MeV. Details of the polarimeter performance and its calibration are given in Ref. [34]. To improve the response function of the polarimeter, the sectored Ge crystal was surrounded by an eightfold-segmented BGO anti-Compton shield, as described previously [32].

III. RESULTS

In Fig. 1 the results of the present NRF experiment on ^{144}Nd including linear polarization measurements of the

scattered photons are summarized. The upper part (a) shows the spectrum of scattered photons detected by the Ge polarimeter installed at an angle of 98° . The high quality of the spectrum was achieved by surrounding the polarimeter crystal by a BGO anti-Compton shield, which also acts as a very efficient active shield against room and cosmic-ray background [32]. The spectrum is dominated by two peaks near 3.2 MeV and a strong excitation at 2.185 MeV. Peaks marked by “ ^{27}Al ” belong to excitations in the ^{27}Al photon flux monitor [36]. In the middle part (b), the reduced transition widths Γ_0^{red} of the photoexcited levels are depicted [the reduced transition widths are proportional to the reduced transition probabilities $B(E1)\uparrow$ and $B(M1)\uparrow$; see Eqs. (4) and (5)]. For the stronger excitations the parities could be determined and are given in the figure: (+) $M1$ excitations, (–) $E1$ excitations. The weak transitions marked by asterisks (*) correspond to $E2$ transitions, as determined from the angular correlation measurements. The azimuthal asymmetries ε , measured with the Compton polarimeter, are shown in the lower part (c) of the figure. The dashed lines correspond to the asymmetries expected for completely polarized photons and are given by the polarization sensitivity $Q(E_\gamma)$ of the polarimeter [34]. Positive asymmetries correspond to positive-parity ($M1$ or $E2$) excitations, whereas negative asymmetries correspond to $E1$ excitations. Solid squares belong to transitions in ^{144}Nd , and the open diamonds indicate the data points for the nearly unpolarized transitions in ^{27}Al . The agreement of these data with $\varepsilon \approx 0$ illustrates the good instrumental symmetry of the polarimeter [34]. The parities given in the middle part (b) were assigned from the measured asymmetries ε .

The sensitivity of the present experiment, even at lower photon energies, is demonstrated in Fig. 2. Here the spectrum of scattered photons is plotted in the low-energy range

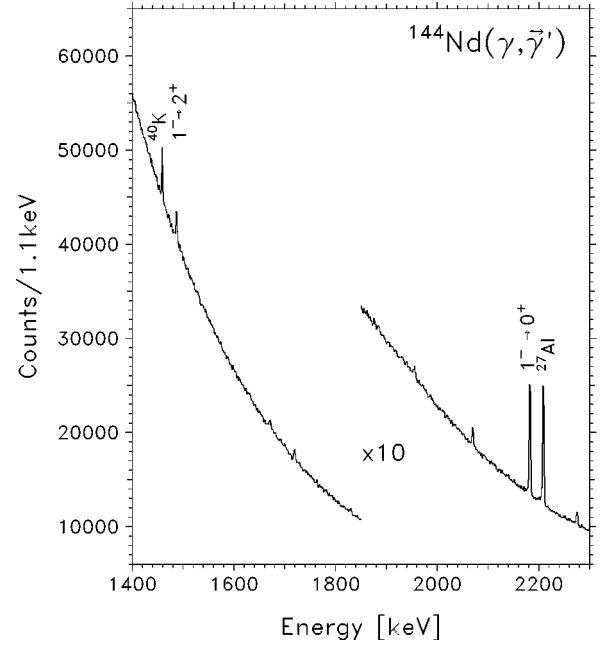


FIG. 2. Low-energy portion of the spectrum of photons scattered from ^{144}Nd measured with the Ge detector at 128° . In the right portion of the spectrum the strong $E1$ transition of the $J^\pi = 1^-$ two-phonon excitation is evident. In the left portion the transition of this 1^- state to the quadrupole phonon 2^+ state clearly can be seen. The ^{27}Al calibration peak and the ^{40}K background peak are labeled.

from 1400 to 2300 keV as measured by the Ge detector at 128° . The ground-state decay of this two-phonon excitation (see Sec. IV) is indicated as $1^- \rightarrow 0^+$. The good sensitivity of the setup enabled us to detect also the decay of this 1^- level to the one-phonon 2^+ state at 696 keV. The corre-

TABLE I. Results of the present $^{144}\text{Nd}(\gamma, \gamma')$ experiment: $M1$ and $E1$ transitions. Excitation energies E_x , integrated cross sections I_s , ground-state decay widths Γ_0 , intensity ratios $W(98^\circ)/W(128^\circ)$, experimental decay branching ratios R_{expt} , azimuthal asymmetries ε , spins and parities J^π , and reduced transition probabilities $B(M1)\uparrow$ and $B(E1)\uparrow$, respectively, are presented.

E_x [keV]	I_s [eVb]	Γ_0 [meV]	$\frac{W(98^\circ)}{W(128^\circ)}$	R_{expt}	ε [%]	Spin/parity J^π	$B(M1)\uparrow$ [μ_N^2]	$B(E1)\uparrow$ [$10^{-3} e^2 \text{fm}^2$]
2072	5.44 ± 0.63	2.03 ± 0.23	1.5 ± 0.3	–	20.0 ± 21.7	1^+	0.059 ± 0.007	–
2185	59.66 ± 4.00	34.61 ± 2.32	0.88 ± 0.14	1.27 ± 0.09	-6.5 ± 3.5	1^-	–	9.51 ± 0.64
2464	1.19 ± 0.40	0.63 ± 0.21	0.47 ± 0.48	–	–	1	0.011 ± 0.004	0.12 ± 0.04
2655	30.55 ± 2.04	23.55 ± 1.58	0.90 ± 0.15	0.65 ± 0.06	0.9 ± 5.7	$(1,2)^{+}$	0.326 ± 0.022	3.61 ± 0.24
2839	1.70 ± 0.40	4.12 ± 0.96	1.27 ± 0.95	5.72 ± 1.71	–	(1)	0.047 ± 0.011	0.52 ± 0.12
2904	8.97 ± 0.74	6.57 ± 0.54	0.73 ± 0.20	–	0.4 ± 18.9	1	0.069 ± 0.006	0.77 ± 0.06
2975	9.59 ± 0.77	15.47 ± 1.24	0.99 ± 0.25	2.45 ± 0.30	-8.2 ± 12.2	1^-	–	1.68 ± 0.14
3213	21.19 ± 1.49	21.90 ± 1.54	0.78 ± 0.15	0.32 ± 0.09	8.7 ± 9.2	1^+	0.171 ± 0.012	–
3244	76.07 ± 5.09	69.43 ± 4.64	0.76 ± 0.12	–	-4.6 ± 4.0	1^-	–	5.83 ± 0.39
3272	1.37 ± 0.48	1.27 ± 0.45	0.92 ± 1.08	–	–	1	0.009 ± 0.003	0.10 ± 0.04
3316	1.34 ± 0.33	1.27 ± 0.31	0.77 ± 0.64	–	–	1	0.009 ± 0.002	0.10 ± 0.03
3486	6.69 ± 0.72	7.06 ± 0.75	0.69 ± 0.26	–	3.5 ± 28.4	1	0.043 ± 0.005	0.48 ± 0.05
3614	23.18 ± 1.85	39.77 ± 3.17	0.67 ± 0.17	0.98 ± 0.15	-9.8 ± 10.7	1^-	–	2.41 ± 0.19
3783	26.55 ± 2.32	32.96 ± 2.89	0.88 ± 0.25	–	1.6 ± 10.5	1	0.158 ± 0.014	1.75 ± 0.15
3838	36.28 ± 3.30	46.38 ± 4.21	0.90 ± 0.26	–	-3.6 ± 9.8	1	0.213 ± 0.019	2.35 ± 0.21
3849	35.09 ± 3.24	48.47 ± 4.48	0.73 ± 0.22	0.14 ± 0.07	4.6 ± 11.2	1	0.220 ± 0.020	2.44 ± 0.23
3860	15.41 ± 1.67	19.92 ± 2.17	0.96 ± 0.37	–	-2.1 ± 17.2	1	0.090 ± 0.010	0.99 ± 0.11

TABLE II. Results of the present $^{144}\text{Nd}(\gamma, \vec{\gamma}')$ experiment: $E2$ transitions. Excitation energies E_x , integrated cross sections I_s , ground-state decay widths Γ_0 , intensity ratios $W(98^\circ)/W(128^\circ)$, experimental decay branching ratios R_{expt} , azimuthal asymmetries ϵ , spins and parities J^π , and reduced transition probabilities $B(E2)\uparrow$ are presented.

E_x [keV]	I_s [eV b]	Γ_0 [meV]	$\frac{W(98^\circ)}{W(128^\circ)}$	R_{expt}	ϵ [%]	Spin/parity J^π	$B(E2)\uparrow$ [$e^2 \text{ fm}^4$]
2527	8.88 ± 0.74	4.09 ± 0.34	1.96 ± 0.53	1.93 ± 0.48	10.0 ± 10.4	2^+	246.0 ± 20.6

sponding 1489 keV transition marked as $1^- \rightarrow 2^+$ is clearly visible above the continuous pulse height distribution from nonresonant scattering of bremsstrahlung photons. The peaks labeled by ^{27}Al and ^{40}K arise from the ^{27}Al photon flux calibration material and the room background, respectively.

The results of the present $^{144}\text{Nd}(\gamma, \vec{\gamma}')$ experiment are summarized in numerical form in Tables I ($E1$ and $M1$ transitions) and II ($E2$ transitions).

IV. DISCUSSION

The dipole strength distribution measured for ^{144}Nd is compared in Fig. 3 with the corresponding distributions in $^{146,148,150}\text{Nd}$ measured in previous NRF experiments [12]. Parity assignments from previous linear polarization experiments [13–15] are also included. The dipole excitations in the transitional nuclei $^{144,146,148}\text{Nd}$ are spread over the entire

energy range 2–4 MeV, and the fragmentation seems to increase with the mass number. On the other hand, in the deformed nucleus ^{150}Nd a cluster of enhanced $M1$ transitions around 3 MeV is evident which can be attributed to the $M1$ scissors mode [13]. The rather strong $E1$ excitation in ^{150}Nd near 2.4 MeV was discussed as a candidate for a new class of two-phonon excitations due to a coupling of the $K=2$ γ vibration and the $K=1$ octupole vibration [37]. Corresponding 1^- states have been systematically observed in several even-even rare earth nuclei [37]. From Fig. 3, in particular, the data for ^{144}Nd and ^{146}Nd , it is clear that both $E1$ and $M1$ excitations are nearly equally distributed in these transitional nuclei. Therefore, unambiguous parity assignments are truly crucial for the interpretation of the observed dipole excitations. This fact clearly emphasizes the necessity for further photon polarization measurements for weaker transitions, in particular when discussing the fragmentation and/or reduced strengths of dipole modes in various mass regions.

A. $E1$ excitation to a quadrupole-octupole coupled 1^- state

The well-known strong $E1$ excitations in the semimagic stable $N=82$ isotones ^{138}Ba , ^{140}Ce , ^{142}Nd , and ^{144}Sm , which are interpreted as excitations of the spin-1 member of the quintuplet from $2^+ \otimes 3^-$ two-phonon coupling, show rather smooth A dependences both of the excitation energy and strength (see, e.g., [7]). The excitation energies, close to the sum of the energies of the quadrupole and octupole phonons, decrease from 4.026 MeV to 3.225 MeV when moving from ^{138}Ba to ^{144}Sm , while the reduced transition probabilities $B(E1)\downarrow$ increase from about 4 to $6 \times 10^{-3} e^2 \text{ fm}^2$. These strengths correspond to about 3–4 mW.u., a value which is more than a factor 30 higher than typical strengths for $E1$ ground-state transitions which are on the order of $10^{-4} - 10^{-8}$ W.u. (1 W.u. equals $64.5A^{2/3} e^2 \text{ fm}^2$). The two-phonon character of these 1^- states in ^{142}Nd [8,9] and ^{144}Sm [9] quite recently was directly proved by $(n, n' \gamma)$ and $(p, p' \gamma)$ experiments where the decay branchings of the two-phonon 1^- states to the one phonon 3^- states could be measured explicitly.

In the $N=84$ nucleus ^{144}Nd , a spin-1 state at 2185 keV has been identified from investigations of ^{144}Pr β decay [38,39]. From these experiments the negative parity of this state was also assigned. The level had already been observed in early photon scattering experiments by Metzger [26]. Its excitation energy is very close to the sum of the 2^+ and 3^- excitations (see Table IV). Information about the other members of the two-phonon quintuplet in ^{144}Nd is perhaps as complete as for any nucleus in this region. In a recent

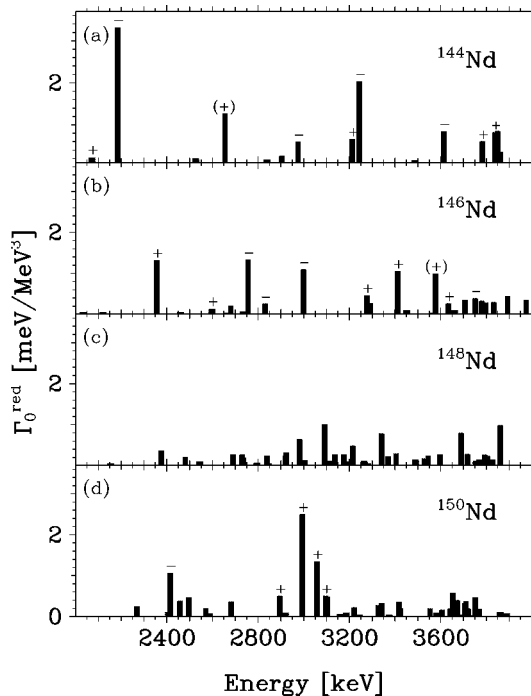


FIG. 3. Systematics of dipole strength distributions in the stable even-even Nd isotopes. Plotted are the reduced ground-state transition widths Γ_0^{red} , which are proportional to the reduced transition probabilities $B(M1)\uparrow$ or $B(E1)\uparrow$, as a function of the excitation energy. Parity assignments from photon polarization measurements are indicated by (+) for $M1$ and by (-) for $E1$ transitions, respectively. In ^{142}Nd , in the shown energy range, a single, very strong $E1$ excitation at 3452 keV ($\Gamma_0 \approx 250$ meV) has been observed in previous NRF work [4,12].

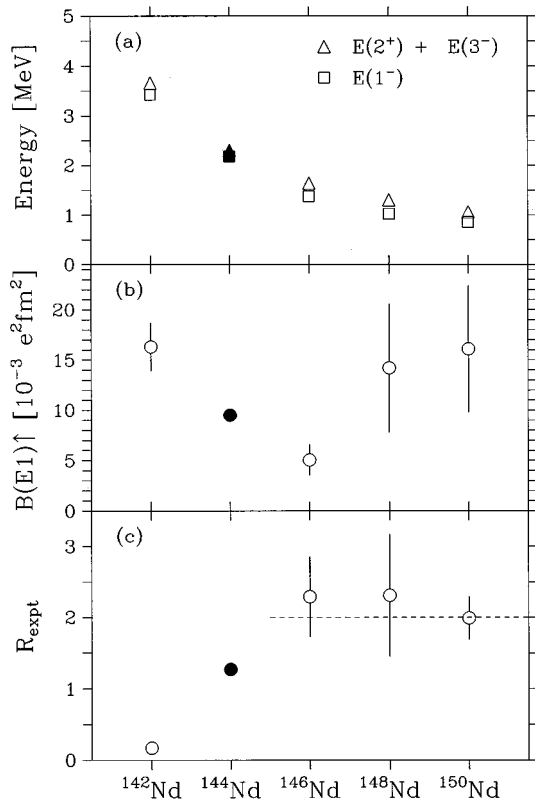


FIG. 4. Systematics of the low-lying 1^- levels in the even- A , stable Nd isotopes. The solid symbols correspond to the new data of the present work. Numerical values and references are given in Table IV. Part (a): excitation energies E_{1^-} compared with the sum of the excitation energies of the first 2^+ and 3^- states. Part (b): reduced excitation probabilities $B(E1)\uparrow$. Part (c): decay branching ratios R_{expt} . The dashed line corresponds to the ratio $R_{\text{expt}} = 2$ as expected from the Alaga rules for well-deformed rotors [48].

(n, γ) experiment, Robinson *et al.* [40] studied the $E2$ and $E3$ transitions of quadrupole-octupole coupled states in ^{144}Nd by measuring the lifetimes of the 1_1^- , 3_1^- , and 5_1^- states using the GRID (gamma-ray induced Doppler broadening [41]) technique. The measured absolute transition rates are consistent with the interpretation of these states as members of the two-phonon quintuplet. While no lifetime could be measured for the 4^- state at 2205 keV, they suggested that this state might also be a member of the quintuplet. Recent lifetime measurements following the $^{144}\text{Nd}(n, n'\gamma)$ reaction [42] indicate that these assignments are correct, and other members of the quintuplet have been identified by the observation of collective $E2$ branches to the 3^- octupole phonon.

Tsoneva, Grinberg, and Stoyanov [43] have recently calculated the $E1$ properties of the even-even $N = 84$ isotones with the QPM. The calculated energies and transition probabilities of the low-lying states in ^{144}Nd are in reasonable agreement with the experimental values, indicating that the main components in the wave functions are well reproduced by the QPM. Moreover, they have calculated the decay characteristics of the negative-parity excitations and determine the 1_1^- state to be primarily of $2^+ \otimes 3^-$ two-phonon character, with the effect of the GDR being to increase the strength of the $E1$ decay to the ground state. On the other hand, the

$E1$ transition strength to the 2_1^+ state is predicted to be rather small [43].

In Table III the decay properties of the 1^- level at 2185 keV in ^{144}Nd as determined in the present NRF study and in previous (γ, γ') and (n, γ) experiments [26,40] are compared with QPM calculations [43]. The experimentally observed ground-state transition probabilities $B(E1)\downarrow(1^- \rightarrow 0^+)$ are in an excellent agreement. QPM calculations [43] also predict the correct magnitude of the strength. The transition probabilities to the first 2^+ state $B(E1)\downarrow(1^- \rightarrow 2^+)$ measured in all experiments are in good agreement, and hence the decay branching ratios R_{expt} are consistent.² However, the QPM calculations [43] fail to reproduce the decay branchings within an order of magnitude. A similar situation exists for the $N = 82$ isotones where the QPM calculations [22] provide a reasonable description of the ground-state transition probabilities of the 1^- two-phonon excitations, but underestimate significantly the branchings to the 2^+ one-phonon state (see [22] and [8,9]).

In Fig. 4 (see also Table IV) the properties of the 1^- state at 2185 keV in ^{144}Nd are compared with those of the corresponding low-lying 1^- states in the stable, even- A Nd nuclei. The new data for ^{144}Nd are shown as solid symbols while open symbols correspond to data from previous Stuttgart NRF work [12]. In the upper part the excitation energies of the first 1^- states are plotted for $^{142,144,146,148,150}\text{Nd}$ and are compared with the sum of the excitation energies of the lowest quadrupole (2^+) and octupole (3^-) excitations, respectively. As for the $N = 82$ isotones (see [7]), with increasing proton number, the 1^- energies follow very closely the sum energy in this isotopic chain with increasing neutron number. The excitation energy of the 1^- state in ^{144}Nd fits very well into this systematics.

In the middle portion of Fig. 4 the reduced excitation probabilities $B(E1)\uparrow$ for the first 1^- states in the stable, even Nd isotopes are depicted. The strength drops when moving from the semimagic ^{142}Nd to the transitional nuclei $^{144,146}\text{Nd}$ and increases when reaching the deformed nucleus ^{150}Nd . The same trend was observed in the Sm isotopic chain [3] and was discussed much earlier by Metzger [4]. This general behavior of the $E1$ strength as a function of the neutron number persists even if the strengths of the corresponding 1^- states in even-even nuclei of different isotopic chains near the closed $N = 82$ shell (Ba, Ce, Nd, Sm chains) [3,45] are considered. The largest strengths were observed for the two-phonon excitations in the spherical $N = 82$ isotones and the deformed nuclei far from the shell closure where the lowest 1^- state corresponds to the bandhead of the $K = 0$ octupole band [46]. The strengths of these excitations could be qualitatively explained by an admixture of the electric giant dipole resonance into these low-lying 1^- states [47].

In the lower panel of Fig. 4, the branching ratios R_{expt} are shown for the even- A Nd isotopes. For spherical ^{142}Nd the

²In the original (n, γ) work [40] an incorrect branching ratio was used in the evaluation of the transition probabilities. In the table the corrected values [44] as communicated by the authors of Ref. [40] are quoted.

TABLE III. Decay properties of the 1^- level at 2185 keV in ^{144}Nd , reduced transition probabilities $B(E1)\downarrow$, and branching ratios R . A comparison of experimental data with QPM calculations is made.

Data	$B(E1)\downarrow (1^- \rightarrow 0^+)$ [$10^{-3} e^2 \text{ fm}^2$]	$B(E1)\downarrow (1^- \rightarrow 2^+)$ [$10^{-3} e^2 \text{ fm}^2$]	R	Reference
(n, γ)	2.4 ± 0.5	3.1 ± 0.7	1.29 ± 0.40	[40,44] ^a
(γ, γ')	2.8 ± 0.4	3.8 ± 0.5	1.36 ± 0.26	[26]
$(\gamma, \tilde{\gamma}')$	3.17 ± 0.21	4.03 ± 0.66	1.27 ± 0.09	this work
QPM	1.95	0.21	0.11	[43]

^aIn their original work [40] an incorrect branching ratio was used in the evaluations. In the present table the corrected values are quoted [44].

branching ratio was too low to be measured in previous NRF experiments [12]. However, recent $(n, n' \gamma)$ and $(p, p' \gamma)$ studies succeeded in detecting the decay branch to the 2^+ vibrational state [8,9]. In ^{144}Nd this transition to the 2^+ state is stronger and was observed both in the present NRF experiment and a previous (n, γ) work [40]. The measured branching ratio fully fits into the systematics of an increasing branching ratio up to a saturation value of $R_{\text{expt}} = 2$, as expected for $K = 0$, $J^\pi = 1^-$ states in deformed nuclei within the validity of the Alaga rules [48]. This expectation value is indicated by the dashed line in the figure.

The data on which Fig. 4 is based are presented in numerical form in Table III.

B. $M1$ excitations of the scissors mode

One of the characteristics of the $M1$ scissors mode is a proportionality of the total $B(M1)$ strength to the square of the deformation parameter (β_2 or δ ; for definitions see [1,2]), and hence to the $B(E2)$ quadrupole strength. The δ^2 dependence of orbital $M1$ strength originally was suggested by macroscopic models [49,50], and the report of its experimental observation in the Sm isotopes [10] initiated a series of theoretical papers. In the meantime various nuclear models, such as microscopic, algebraic, geometrical, and phenomenological, were used to explain the quadratic dependence of the total $M1$ strength on the nuclear deformation [51–62]. The “ δ^2 law” also is consistent with the observed saturation of the strength in the midshell mass region of the rare earth nuclei [63]. Also, recently derived sum rules for the orbital $M1$ strength explicitly contain the proportionality to the square of the deformation parameter δ or β_2 [56,64].

The deformation parameter β_2 is directly connected to the reduced transition probability $B(E2, 0^+ \rightarrow 2^+)$ and the quadrupole moment Q_0 :

$$\beta_2 = \frac{4\pi}{3ZR_0^2} \sqrt{\frac{B(E2, 0^+ \rightarrow 2^+)}{e^2}} = \frac{4\pi}{3ZR_0^2} \sqrt{\frac{5}{16\pi}} Q_0, \quad (9)$$

where Z represents the atomic number and R_0 corresponds to $1.2 \text{ fm } A^{1/3}$. In this article, the deformation parameter β_2 will be used since it is directly determined from measured $B(E2)$ values.

In a recent compilation of all available NRF data on the $M1$ scissors mode strength, Pietralla *et al.* [65] demonstrated the existence of a striking correlation between the low-lying $M1$ and $E2$ strengths not only for the transition from spherical to deformed nuclei but also for heavier rare earth nuclei where a transition occurs to γ -soft, so-called O(6) nuclei. Results from recent NRF experiments on γ -soft nuclei ^{196}Pt [66], the best known O(6) nucleus, and ^{134}Ba [67] and the transitional, heavy nuclei $^{178,180}\text{Hf}$ [68] and $^{190,192}\text{Os}$ [69] confirmed the expected reduced total $M1$ strength and fit well into the systematics of the proportionality of $B(M1)$ and $B(E2)$ strength [70].

As noted earlier, experimental evidence for the so-called “ δ^2 law” was first reported by the Darmstadt group for the even- A Sm isotopes [10,11]. First NRF experiments on the stable even- A Nd isotopes $^{142,146,148,150}\text{Nd}$ [12] subsequently were completed with polarization experiments on $^{142,146,150}\text{Nd}$ [13,14,16] to establish definite parity assignments for the observed dipole excitations. The parity determinations are crucial for the extraction of total strengths and

TABLE IV. Comparison of the properties of the low-lying 1^- levels in the even- A , stable Nd isotopes. Excitation energies, reduced excitation probabilities $B(E1)\uparrow$, and decay branchings R_{expt} are given.

Isotope	E_{2^+} [MeV]	E_{3^-} [MeV]	$E_{2^+} + E_{3^-}$ [MeV]	E_{1^-} [MeV]	$B(E1)\uparrow$ [$10^{-3} e^2 \text{ fm}^2$] ^a	R_{expt}	Reference
^{142}Nd	1.576	2.084	3.660	3.425	16.3 ± 2.4	0.17 ± 0.03 ^b	[12]
^{144}Nd	0.696	1.511	2.207	2.185	9.51 ± 0.64	1.27 ± 0.09	this work
^{146}Nd	0.454	1.190	1.644	1.377	5.05 ± 1.54	2.29 ± 0.56	[12]
^{148}Nd	0.302	1.000	1.302	1.023	14.2 ± 6.4	2.31 ± 0.86	[12]
^{150}Nd	0.130	0.930	1.060	0.853	16.1 ± 6.3	1.99 ± 0.30	[12]

^a $B(E1)_{\text{W.u.}} = 64.5A^{2/3} e^2 \text{ fm}^2$; e.g., for $A=144$, $1 \text{ W.u.} = 1.772 e^2 \text{ fm}^2$.

^bFrom Refs. [8,9].

for comparisons with sum rules, particularly for transitional nuclei where $M1$ and $E1$ excitations occur with comparable strengths (see Fig. 3). For these nuclei, which are not good rotors, the Alaga rule is not valid and positive parity based on observed $K=1$ assignments is very questionable. Furthermore, the dipole strength in these nuclei is quite fragmented. Therefore, when discussing the total strength, e.g., of *scissors mode* excitations, the absolute numbers to be compared depend on the assumption of the energy range over which the strength can be fragmented. In the compilation of Ref. [65] showing the correlation between the low-lying $M1$ and $E2$ strengths in rare earth nuclei, integration intervals for the *scissors mode* of 2.7–3.7 MeV and 2.4–3.7 MeV were chosen consistently for light and heavy rare earth nuclei, respectively. In this paper we integrate over the 2.7–3.7 MeV range to provide a consistent comparison with the systematics discussed in Ref. [65]. It should be noted that in previous work [16,17] we gave numbers obtained for the larger energy range of 2–4 MeV.

Figure 5 shows the integrated $B(M1)\uparrow$ in the even-even Nd isotopes $^{142,144,146,148,150}\text{Nd}$ (integration interval 2.7–3.7 MeV) as a function of the square of the deformation parameter β_2 . As discussed earlier, we prefer to use the deformation parameter β_2 instead of δ because β_2 is directly connected to the experimentally accessible reduced transition probability $B(E2)$ and is proportional to the quadrupole moment [see Eq. (9)]. Solid symbols in Fig. 5 correspond to $M1$ strengths of transitions with reliable parity assignments from linear polarization measurements, including the results of the present experiments; open symbols correspond to total strengths obtained by summing the strengths of all dipole transitions in the energy range of interest ($E_\gamma=2.7\text{--}3.7$ MeV) showing a $R_{\text{expt}}\leq 1$ decay branching. Consideration of all $\Delta K=1$ transitions in the energy range of interest (open squares), which seems to be reasonable in the case of the well-deformed nucleus ^{150}Nd , obviously leads to remarkable overall agreement with the Darmstadt Sm results [10]. Moreover, the linear dependence of the data shown in Fig. 5 is clear. It should be noted that the slope of the linear dependence can be influenced by the experimental detection sensitivity (number of weak transitions of unknown parities included in the sums); however, large changes are not anticipated due to the increased sensitivity achieved in modern NRF experiments.

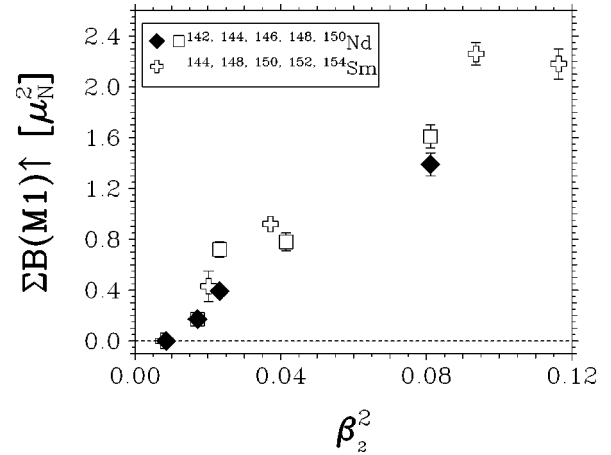


FIG. 5. The total $M1$ strengths observed in the even- A Nd isotopes in the energy range 2.7–3.7 MeV as a function of the square of the deformation parameter β_2 (data from Margraf *et al.* [16] and the present work). Solid symbols: only transitions in Nd isotopes with parities known from NRF polarization measurements have been included. Open squares: summed strengths of all transitions from spin-1 states with decay branching ratios $R_{\text{expt}}\leq 1$ corresponding to $K=1$ states within the validity of the Alaga rules. Open crosses: data observed by the Darmstadt group for the even- A Sm isotopes (Ziegler *et al.*, [10]).

Obviously, the new data for ^{144}Nd fit well into the systematics of the total $M1$ strengths in the even- A Nd isotopes, and these results represent a reliable independent confirmation of the “ δ^2 law” [10]. As noted previously, this δ^2 or β_2^2 dependence of the $M1$ *scissors mode* strengths, and hence the proportionality between $B(M1)$ and $B(E2)$ strengths, has been explained in the framework of a diversity of theoretical models [51–62].

ACKNOWLEDGMENTS

We wish to thank Ch. Stoyanov, S.F. Hicks, and J.R. Vanhoy for providing us with the results of their work prior to publication. We are grateful to S.J. Robinson and K.P. Lieb for clarifying discussions. Support by the Deutsche Forschungsgemeinschaft under Contracts Nos. Br 799/6, Kn 154/21, and Kn 154/30 and by the U.S. National Science Foundation under Grant No. PHY-9515461 is gratefully acknowledged.

- [1] K.E.G. Löbner, M. Vetter, and V. Hönl, Nucl. Data, Sect. A **7**, 495 (1970).
- [2] S. Raman, C.H. Malarkey, W.T. Milner, C.W. Nestor, Jr., P.H. Stelson, At. Data Nucl. Data Tables **36**, 1 (1987).
- [3] F.R. Metzger, Phys. Rev. C **14**, 543 (1976).
- [4] F.R. Metzger, Phys. Rev. C **18**, 1603 (1978).
- [5] F.R. Metzger, Phys. Rev. C **18**, 2138 (1978).
- [6] R.A. Gatenby, J.R. Vanhoy, E.M. Baum, E.L. Johnson, S.W. Yates, T. Belgia, B. Fazekas, Á. Veres, and G. Molnár, Phys. Rev. C **41**, R414 (1990).
- [7] R.-D. Herzberg, I. Bauske, P. von Brentano, Th. Eckert, R. Fischer, W. Geiger, U. Kneissl, J. Margraf, H. Maser, N. Pi-

etralla, H.H. Pitz, and A. Zilges, Nucl. Phys. **A592**, 211 (1995).

- [8] T. Belgia, R.A. Gatenby, E.M. Baum, E.L. Johnson, D.P. DiPrete, S.W. Yates, B. Fazekas, and G. Molnár, Phys. Rev. C **52**, R2314 (1995).
- [9] M. Wilhelm, E. Rademacher, A. Zilges, and P. von Brentano, Phys. Rev. C **54**, R449 (1996); M. Wilhelm, S. Kasemann, G. Pascovici, E. Rademacher, A. Zilges, and P. von Brentano (private communication).
- [10] W. Ziegler, C. Rangacharyulu, A. Richter, and C. Spieler, Phys. Rev. Lett. **65**, 2515 (1990).
- [11] W. Ziegler, N. Huxel, P. von Neumann-Cosel, C. Ranga-

- charyulu, A. Richter, C. Spieler, C. De Coster, and K. Heyde, Nucl. Phys. **A564**, 366 (1993).
- [12] H.H. Pitz, R.D. Heil, U. Kneissl, S. Lindenstruth, U. Seemann, C. Wesselborg, A. Zilges, P. v. Brentano, S.D. Hoblit, and A.M. Nathan, Nucl. Phys. **A509**, 587 (1990).
- [13] B. Kasten, R.D. Heil, P. v. Brentano, P.A. Butler, S.D. Hoblit, U. Kneissl, S. Lindenstruth, G. Müller, H.H. Pitz, K.W. Rose, W. Scharfe, M. Schumacher, U. Seemann, Th. Weber, C. Wesselborg, and A. Zilges, Phys. Rev. Lett. **63**, 609 (1989).
- [14] R.D. Heil, B. Kasten, W. Scharfe, P.A. Butler, H. Friedrichs, S.D. Hoblit, U. Kneissl, S. Lindenstruth, M. Ludwig, G. Müller, H.H. Pitz, K.W. Rose, M. Schumacher, U. Seemann, J. Simpson, P. v. Brentano, Th. Weber, C. Wesselborg, and A. Zilges, Nucl. Phys. **A506**, 223 (1990).
- [15] H. Friedrichs, B. Schlitt, J. Margraf, S. Lindenstruth, C. Wesselborg, R.D. Heil, H.H. Pitz, U. Kneissl, P. von Brentano, R. D. Herzberg, A. Zilges, D. Häger, G. Müller, and M. Schumacher, Phys. Rev. C **45**, R892 (1992).
- [16] J. Margraf, R.D. Heil, U. Maier, U. Kneissl, H.H. Pitz, H. Friedrichs, S. Lindenstruth, B. Schlitt, C. Wesselborg, P. von Brentano, R.-D. Herzberg, and A. Zilges, Phys. Rev. C **47**, 1474 (1993).
- [17] U. Kneissl, H.H. Pitz, and A. Zilges, Prog. Part. Nucl. Phys. **37**, 349 (1996).
- [18] U.E.P. Berg and U. Kneissl, Annu. Rev. Nucl. Part. Sci. **37**, 33 (1987).
- [19] P.O. Lipas, Nucl. Phys. **82**, 91 (1966).
- [20] P. Vogel and L. Kocbach, Nucl. Phys. **A176**, 33 (1971).
- [21] V.V. Voronov, D.T. Khoa, and V.Yu. Ponomarev, Bull. Acad. Sci. USSR, Phys. Ser. **48** (9), 190 (1984).
- [22] M. Grinberg and Ch. Stoyanov, Nucl. Phys. **A573**, 231 (1994).
- [23] K. Govaert, L. Govor, E. Jacobs, D. De Frenne, W. Mondelaers, K. Persyn, M.-L. Yoneama, U. Kneissl, J. Margraf, H.H. Pitz, K. Huber, S. Lindenstruth, R. Stock, K. Heyde, A. Vdovin, and V.Yu. Ponomarev, Phys. Lett. B **335**, 113 (1994).
- [24] K. Heyde and C. De Coster, Phys. Lett. B **393**, 7 (1997).
- [25] R.-D. Herzberg, P. von Brentano, J. Eberth, J. Enders, L. Esser, R. Fischer, N. Huxel, T. Klemme, P. von Neumann-Cosel, N. Nicolay, N. Pietralla, V.Yu. Ponomarev, J. Reif, A. Richter, C. Schlegel, R. Schwengner, S. Skoda, H.G. Thomas, I. Wiedenhöver, G. Winter, and A. Zilges, Phys. Lett. B **390**, 49 (1997).
- [26] F.R. Metzger, Phys. Rev. **187**, 1700 (1969).
- [27] N. Lo Iudice and F. Palumbo, Phys. Rev. Lett. **41**, 1532 (1978).
- [28] D. Bohle, A. Richter, W. Steffen, A.E.L. Dieperink, N. Lo Iudice, F. Palumbo, and O. Scholten, Phys. Lett. **137B**, 27 (1984).
- [29] A. Richter, Prog. Part. Nucl. Phys. **34**, 261 (1995).
- [30] P. Carlos, H. Beil, R. Bergère, A. Leprêtre, and A. Veyssièrre, Nucl. Phys. **A172**, 437 (1971).
- [31] P. Carlos, H. Beil, R. Bergère, A. Leprêtre, A. de Miniac, and A. Veyssièrre, Nucl. Phys. **A225**, 171 (1974).
- [32] H. Maser, S. Lindenstruth, I. Bauske, O. Beck, P. von Brentano, T. Eckert, H. Friedrichs, R.D. Heil, R.-D. Herzberg, A. Jung, U. Kneissl, J. Margraf, N. Pietralla, H.H. Pitz, C. Wesselborg, and A. Zilges, Phys. Rev. C **53**, 2749 (1996).
- [33] A. Nord, A. Schiller, T. Eckert, O. Beck, J. Besserer, P. von Brentano, R. Fischer, R.-D. Herzberg, D. Jäger, U. Kneissl, J. Margraf, H. Maser, N. Pietralla, H.H. Pitz, M. Rittner, and A. Zilges, Phys. Rev. C **54**, 2287 (1996).
- [34] B. Schlitt, U. Maier, H. Friedrichs, S. Albers, I. Bauske, P. von Brentano, R.D. Heil, R.-D. Herzberg, U. Kneissl, J. Margraf, H.H. Pitz, C. Wesselborg, and A. Zilges, Nucl. Instrum. Methods Phys. Res. A **337**, 416 (1994).
- [35] J. Margraf, T. Eckert, M. Rittner, I. Bauske, O. Beck, U. Kneissl, H. Maser, H.H. Pitz, A. Schiller, P. von Brentano, R. Fischer, R.-D. Herzberg, N. Pietralla, A. Zilges, and H. Friedrichs, Phys. Rev. C **52**, 2429 (1995).
- [36] N. Pietralla, I. Bauske, O. Beck, P. von Brentano, W. Geiger, R.-D. Herzberg, U. Kneissl, J. Margraf, H. Maser, H.H. Pitz, and A. Zilges, Phys. Rev. C **51**, 1021 (1995).
- [37] U. Kneissl, A. Zilges, J. Margraf, I. Bauske, P. von Brentano, H. Friedrichs, R.D. Heil, R.-D. Herzberg, H.H. Pitz, B. Schlitt, and C. Wesselborg, Phys. Rev. Lett. **71**, 2180 (1993).
- [38] S. Raman, Nucl. Data, Sect. B **2**, 47 (1967).
- [39] S. Raman, Nucl. Phys. **A107**, 402 (1968).
- [40] S.J. Robinson, J. Jolie, H.G. Börner, P. Schillebeeckx, S. Ulbig, and K.P. Lieb, Phys. Rev. Lett. **73**, 412 (1994).
- [41] H.G. Börner and J. Jolie, J. Phys. G **19**, 217 (1993).
- [42] J.R. Vanhoy and S.F. Hicks (private communication); (unpublished).
- [43] N. Tsoneva, M. Grinberg, and Ch. Stoyanov (private communication); (unpublished).
- [44] S.J. Robinson (private communication).
- [45] H.H. Pitz, Ph.D. thesis, Giessen, 1989.
- [46] A. Zilges, P. von Brentano, H. Friedrichs, R.D. Heil, U. Kneissl, S. Lindenstruth, H.H. Pitz, and C. Wesselborg, Z. Phys. A **340**, 155 (1991).
- [47] A. Zilges, P. von Brentano, and A. Richter, Z. Phys. A **341**, 489 (1992).
- [48] G. Alaga, K. Alder, A. Bohr, and B.R. Mottelson, K. Dan. Vidensk. Selsk. Mat. Fys. Medd. **29**, No. 9, 1 (1955).
- [49] S.G. Rohozński and W. Greiner, Z. Phys. A **322**, 271 (1985).
- [50] R. Nojarov, Z. Bochnacki, and A. Faessler, Z. Phys. A **324**, 289 (1986).
- [51] I. Hamamoto and C. Magnusson, Phys. Lett. B **260**, 6 (1991).
- [52] E. Garrido, E. Moya de Guerra, P. Sarriguren, and J.M. Udías, Phys. Rev. C **44**, R1250 (1991).
- [53] T. Mizusaki, T. Otsuka, and M. Sugita, Phys. Rev. C **44**, R1277 (1991).
- [54] J.N. Ginocchio, Phys. Lett. B **265**, 6 (1991).
- [55] L. Zamick and D.C. Zheng, Phys. Rev. C **46**, 2106 (1992).
- [56] N. Lo Iudice and A. Richter, Phys. Lett. B **304**, 193 (1993).
- [57] K. Heyde, C. De Coster, D. Ooms, and A. Richter, Phys. Lett. B **312**, 267 (1993).
- [58] R.R. Hilton, W. Höhenberger, and H.J. Mang, Phys. Rev. C **47**, 602 (1993).
- [59] E. Moya de Guerra and L. Zamick, Phys. Rev. C **47**, 2604 (1993).
- [60] P. Sarriguren, E. Moya de Guerra, R. Nojarov, and A. Faessler, J. Phys. G **20**, 315 (1994).
- [61] N. Lo Iudice, A.A. Raduta, and D.S. Delion, Phys. Rev. C **50**, 127 (1994).
- [62] B.H. Smith, X.W. Pan, D.H. Feng, and M. Guidry, Phys. Rev. Lett. **75**, 3086 (1995).
- [63] C. Rangacharyulu, A. Richter, H.J. Wörtche, W. Ziegler, and R.F. Casten, Phys. Rev. C **43**, R949 (1991).
- [64] P. von Neumann-Cosel, J.N. Ginocchio, H. Bauer, and A. Richter, Phys. Rev. Lett. **75**, 4178 (1995).
- [65] N. Pietralla, P. von Brentano, R.-D. Herzberg, A. Zilges, U.

- Kneissl, J. Margraf, H. Maser, and H.H. Pitz, *Phys. Rev. C* **52**, R2317 (1995).
- [66] P. von Brentano, J. Eberth, J. Enders, L. Esser, R.-D. Herzberg, N. Huxel, M. Meise, P. von Neumann-Cosel, N. Nicolay, N. Pietralla, H. Prade, J. Reif, A. Richter, C. Schlegel, R. Schwengner, S. Skoda, H.G. Thomas, I. Wiedenhöver, G. Winter, and A. Zilges, *Phys. Rev. Lett.* **76**, 2029 (1996).
- [67] H. Maser, N. Pietralla, P. von Brentano, R.-D. Herzberg, U. Kneissl, J. Margraf, H.H. Pitz, and A. Zilges, *Phys. Rev. C* **54**, R2129 (1996).
- [68] N. Pietralla, O. Beck, J. Besserer, P. von Brentano, T. Eckert, R. Fischer, C. Fransen, R.-D. Herzberg, D. Jäger, R.V. Jolos, U. Kneissl, B. Krischok, J. Margraf, H. Maser, A. Nord, H.H. Pitz, M. Rittner, A. Schiller, and A. Zilges, *Nucl. Phys.* **A618**, 141 (1997).
- [69] B. Krischok, Diploma thesis, Stuttgart 1996; C. Fransen, Diploma thesis, Köln 1997; (unpublished).
- [70] N. Pietralla, C. Fransen, P. von Brentano, R.-D. Herzberg, A. Zilges, O. Beck, J. Besserer, T. Eckert, D. Jäger, U. Kneissl, B. Krischok, H. Maser, J. Margraf, A. Nord, and H.H. Pitz, in *Proceedings of the 9th International Symposium on "Capture Gamma-Ray Spectroscopy and Related Topics,"* Budapest, Hungary, 1996, edited by E. Molnár (Springer-Verlag, Budapest, 1997).